Scattering effects in surface wave tomography by membrane waves

Summary: In order to conduct seismic tomography, one might use the most adequate description of wave propagation; thus far, almost all tomographic models rely on ray theory, a high-frequency approximation. Particularly for surface waves, Born theory, a single scattering theory, improves it by taking first order scattering effects into account. The resulting sensitivity kernels are typically derived from analytical far-field Green's tensors, which lead to singularities at source and receiver locations; numerical derivation of kernels in contrast can avoid this, but full numerical integration of the equations of motion in 3D is expensive. For surface waves, the membrane wave method restricts the propagation to two dimensions; it allows thus to compute numerical sensitivity kernels in a shorter time. We investigate the potential of the membrane wave method to produce a kernel library for tomographic algorithms and compare our results with linear approximation theories.

Meshing of the Earth's surface

Discretization takes advantage of geodesic grids initially found for meteorological flow modelling.

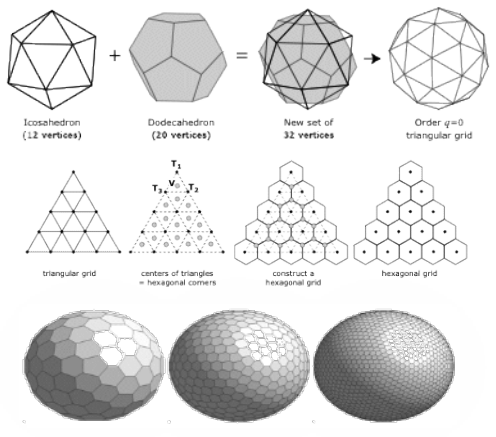

Fig. 1: Spherical grid construction uses initially the icosahedron & dodecahedron vertices. Refinement is done by subfolding corresponding triangles (Tape, 2003)

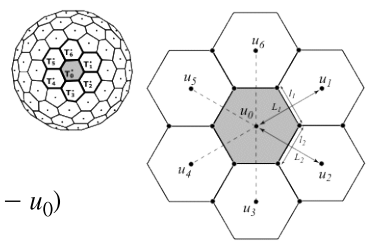

$$\nabla^2 u\,|_{T_0} \approx \frac{1}{A_0}\sum_{i=1}^{N}\frac{l_i}{L_i}(u_i - u_0)$$

Fig. 2: Finite-difference scheme using cell area, center distances and cell edge lengths expresses the Laplacian on a spherical grid (Heikes&Randall, 1995; Tape, 2003).

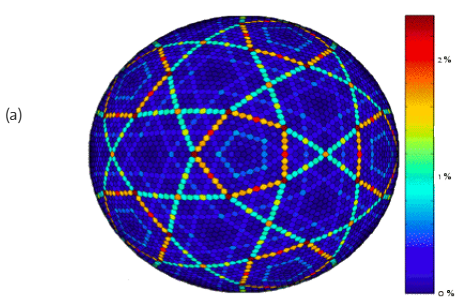

Fig. 3: Accuracy of Laplacian is influenced by grid distortion. (a) Cell distortion is induced by the subfolding method. (b) Differences to analytical solution for a spherical harmonic function (L=6,M=1) are still small compared to the maximum analytical Laplacian.

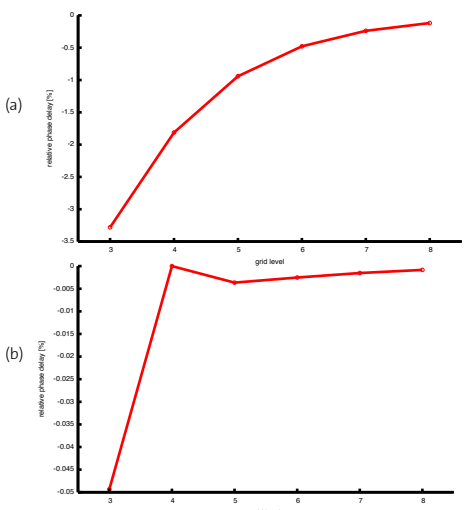

Fig. 4: Error of the (a) unfiltered and (b) filtered numerical solution for different levels of grid refinement, compared with the analytical solution (see Fig. 10) in terms of relative phase delay. Filtering is done around the corner frequency for Love waves at 150 s. Notice that the numerical displacements arrive earlier (negative delays) compared to the analytical ones.

Numerical sensitivity functions

Let us introduce the "Born" sensitivity function $K(\vartheta,\varphi)$ such that

$$\delta\Phi = \int_{\Omega} K(\vartheta,\varphi,\omega)\,\delta v(\vartheta,\varphi,\omega)\,d\Omega$$

We perform a set of simulations with phase velocity

$$\delta v(\vartheta,\varphi) = \begin{cases} 0 & \text{everywhere} \\ 1 & \text{within cell centered at } (\vartheta_i,\varphi_i) \text{ and area } A_i \end{cases}$$

$\delta\Phi_i(\omega)$ is found by cross-correlation & filtering around ω. The Kernel values at each cell location are given by

$$K(\vartheta_i,\varphi_i,\omega) = \frac{\delta\Phi_i}{A_i}$$

Numerical vs. analytical kernels

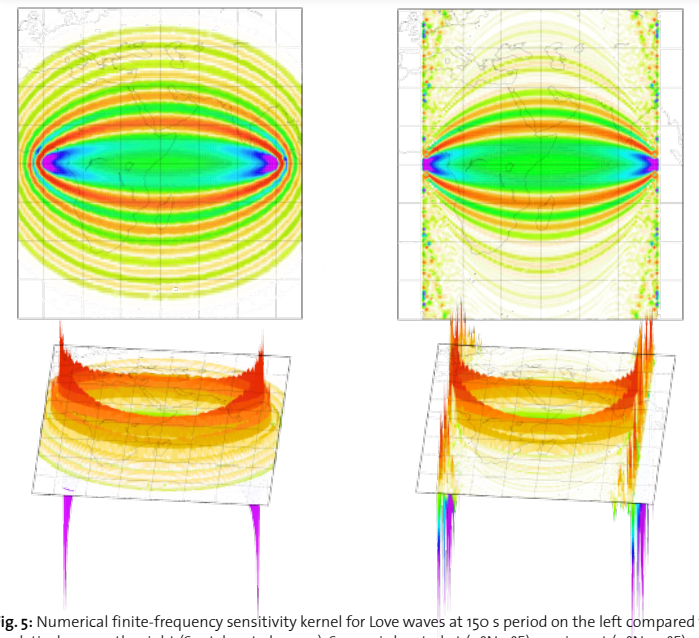

Fig. 5: Numerical finite-frequency sensitivity kernel for Love waves at 150 s period on the left compared to analytical one on the right (Spetzler et al., 2002). Source is located at (0°N,0°E), receiver at (0°N,90°E).

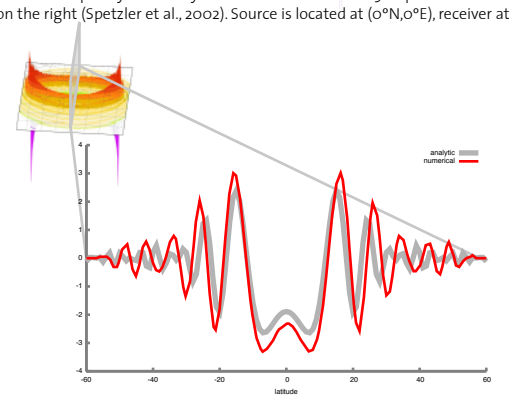

Fig. 6: Kernels of Fig. 8 plotted at 45° longitude, as a function of latitude.

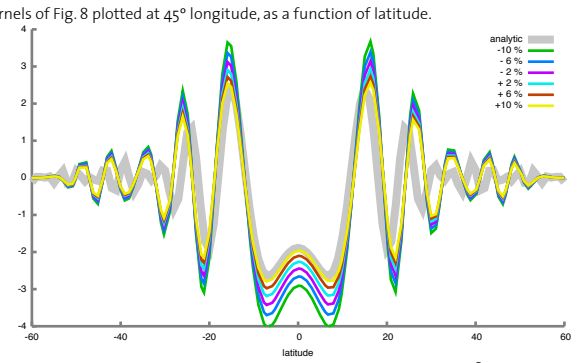

Fig. 7: Strange nonlinear effect: the kernel shape is effected by input values of δv. The kernel value converges for sufficiently small δv.

Numerical integration vs. linearized theory

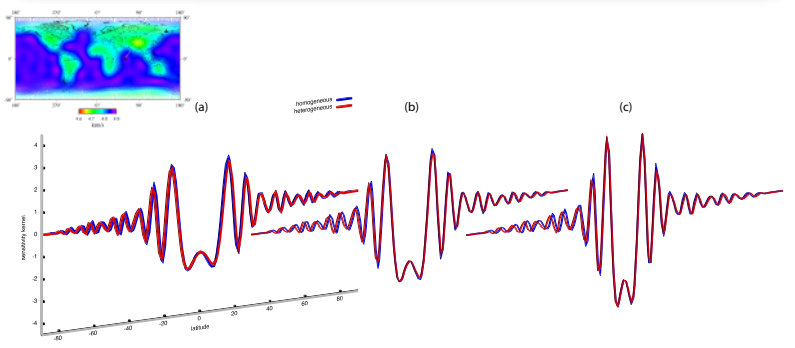

Fig. 8: Effects of a heterogeneous crustal phase velocity map (based on CRUST 2.0; smoothed to harmonic degree 12). Profiles of numerical kernels for 150 s Love waves, taken perpendicular to the source-receiver great circle which crosses the Tibetian anomaly, at epicentral distances of (a) 45°, (b) 70° and (c) 80°.

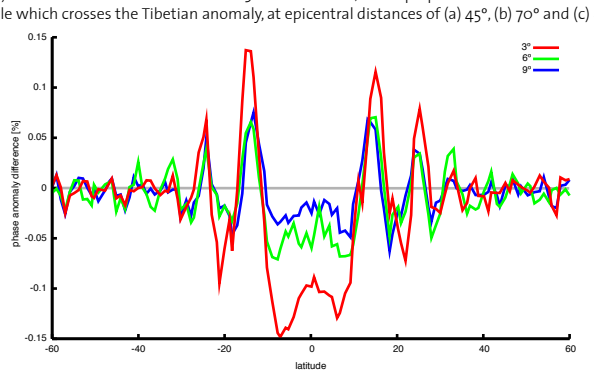

Fig. 9: Combined effect of two scatterers, modeled with a single simulation vs. two independent simulations whose results are then summed. The experiment is repeated for ~100 couples of scatterers located at same latitude, with 3°,6° resp. 9° degrees longitudal distance from each other; source and receiver are as in Fig. 5; first scatterers are at 45° longitude and percent discrepancy in $\delta\Phi$ (normalized to its maximum value given by Born theory) are plotted as a function of latitude.

Membrane waves

(1) $\rho\ddot{\mathbf{u}} = \nabla\cdot\tau + \mathbf{f}$

(2) $\mathbf{u}_L = W(\mathbf{r})(-\hat{\mathbf{r}}\times\nabla_1)\chi(\vartheta,\varphi)$

substituting Love wave ansatz (2) into (1) one finds that with smooth-Earth approximation χ obeys:

(3) $\nabla_1^2\chi = \frac{\omega^2}{\mathbf{c}(\vartheta,\varphi)^2}\chi$

which is valid for each frequency ω (Tanimoto, 1990; Tromp & Dahlen, 1993). We solve (3) in time domain prescribing an initial displacement and "source time function":

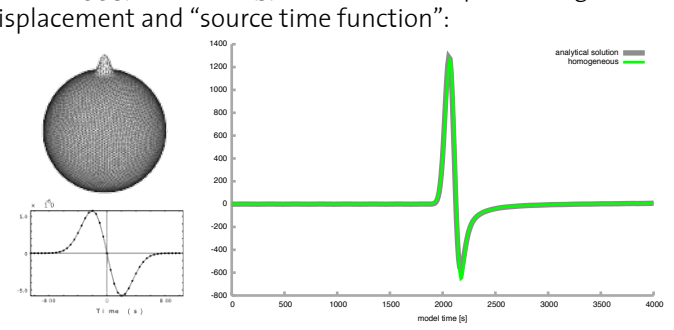

Fig. 10: Comparison can be made between analytical and numerical solution in the case of a homogeneous phase velocity map with a Gaussian initial displacement (in space and time shown on the left).

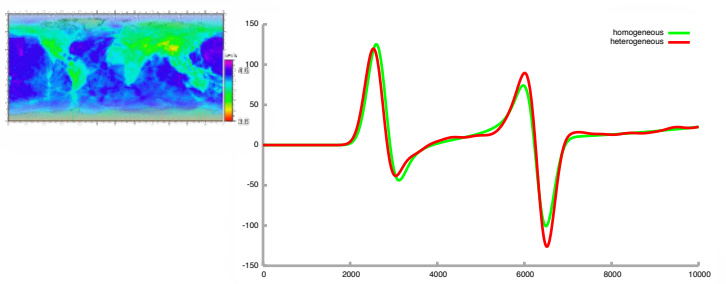

Fig. 11: Differences between solutions using a homogeneous vs. a heterogeneous phase velocity map (for Love waves at 35 s).

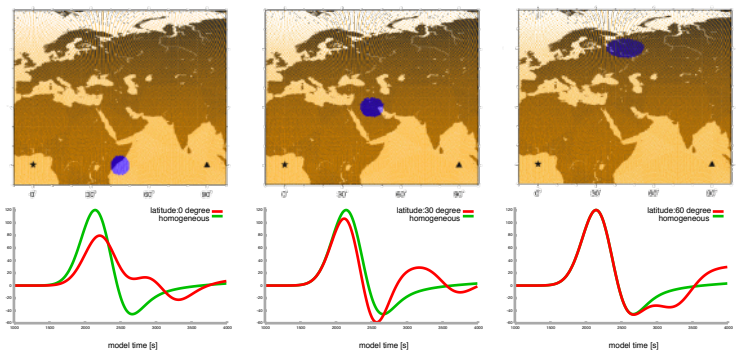

Fig. 12: Scattering effects for lateral heterogeneities (blue circles) depending on their location between source (at 0°N,0°E) and receiver (at 0°N,90°E).

Algorithm's performance

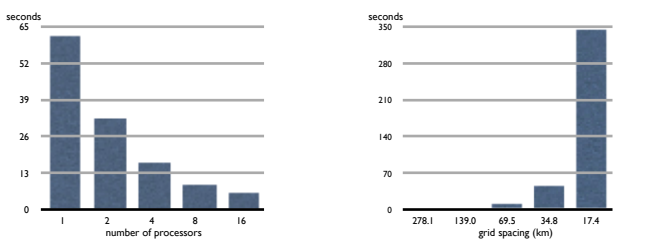

Fig. 13: Benchmarking of the code for Love waves at 150 s period with a propagation time of ~40 min. Calculation times are within seconds and scale well with respect to any cluster size.

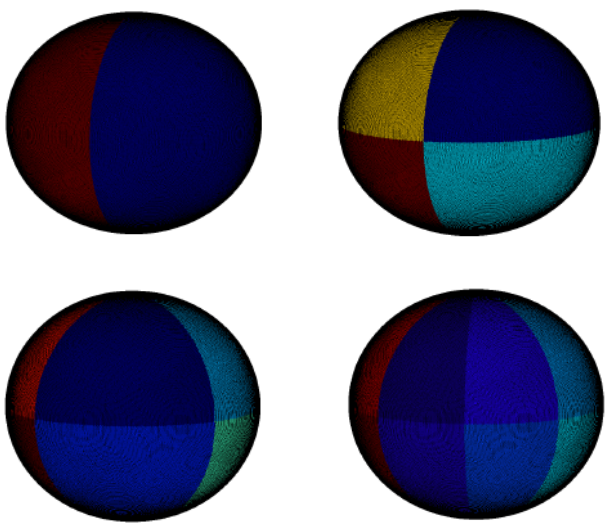

Fig. 14: Spherical grid discretized into domains for parallel computation with 2, 4, 8 and 16 processes.

References:
Heikes R., Randall DA., 1995. Numerical integration of the shallow-water equations on a twisted icosahedral grid. Part I: basic design and results of tests. *Mon. Weather Rev.* 123(6):1862-1880.
Spetzler J., Trampert J., Snieder R., 2002. The effect of scattering in surface wave tomography, *Geophys. J. Int.*, 149, 755-767
Tanimoto T., 1990. Modelling curved surface wave paths: Membrane surface wave synthetics, *Geophys. J. Int.*, 102, 89-100, 1990
Tape C.H., 2003. *Waves on a Spherical Membrane*. M.Sc. thesis, University of Oxford, U.K.
Tromp J., Dahlen F.A., 1993. Variational principles for surface wave propagation on a laterally heterogeneous Earth -III. Potential representation, *Geophys. J. Int.*, 112, 195--209.

D. Peter & L. Boschi, Institute of Geophysics, ETH
(dpeter@erdw.ethz.ch)

Acknowledgements:
John Woodhouse & Carl Tape are thanked for their help & support, Domenico Giardini for his constant support and encouragement, and Yann Capdeville for his many insightful comments. Funding for this project is provided by the European Commission's Human Resources and Mobility Programme Marie Curie Research Training Network SPICE Contract No. MRTN-CT-2003-504267.

ETH
Eidgenössische Technische Hochschule Zürich
Swiss Federal Institute of Technology Zurich